Kohn's localization in disordered fermionic systems with and without interactions

Vipin Kerala Varma and Sebastiano Pilati
The Abdus Salam International Centre for Theoretical Physics, Trieste, Italy
(Received 30 April 2015; published 15 October 2015)

Understanding the metal-insulator transition in disordered many-fermion systems, both with and without interactions, is one of the most challenging and consequential problems in condensed matter physics. In this paper, we address this issue from the perspective of the modern theory of the insulating state (MTIS), which has already proven to be effective for band and Mott insulators in clean systems. First, we consider noninteracting systems with different types of aperiodic external potentials: uncorrelated disorder (one-dimensional Anderson model), deterministic disorder (Aubry-André Hamiltonian and its modification including next-nearest-neighbor hopping), and disorder with long-range correlations (self-affine potential). We show how the many-body localization tensor defined within the MTIS may be used as a powerful probe to discriminate the insulating and the metallic phases, and to locate the transition point. Then, we investigate the effect of weak repulsive interactions in the Aubry-André Hamiltonian, a model which describes a recent cold-atoms experiment. By treating the weak interactions within a mean-field approximation we obtain a linear shift of the transition point towards stronger disorder, providing evidence for delocalization induced by interactions.

DOI: 10.1103/PhysRevB.92.134207 PACS number(s): 71.10.Fd, 71.30.+h, 71.23.An, 72.15.Rn

I. INTRODUCTION

In the modern theory of the insulating state (MTIS), which was initiated by the seminal article written by Kohn [1], the different behaviors of metals and insulators are attributed to the different organizations of the electrons in the many-body ground state. In insulators, the electrons satisfy a many-particle localization condition [2]. Kohn associated this localization with the breakup of the many-electron wave function into terms which are localized in essentially disconnected regions of the many-particle configuration space. This approach is fundamentally different from conventional theories of insulators, which require the knowledge of, at least, low-lying excitations, and are tailored towards a specific kind of insulator, depending on the physical mechanism which triggers the insulating behavior. Some fundamental developments in the MTIS were achieved only in the late 1990s (thanks to the works by Resta and Sorella [3], and others [4,5]). These developments began with the observation that the polarization is finite in insulator, while it is ill defined in metals. This led to a definition of the localization tensor [3] of a many-body system which is derived from the Berry-phase formulation of the polarization as understood within the modern theory of the polarization [6–8]. The direct connection between the many-body localization tensor and the disconnected parts of the many-electron wave function, as originally defined by Kohn, was demonstrated by Souza, Wilkens, and Martins [4].

The MTIS is supposed to be adequate to describe any kind of insulator, independent of the physical mechanism which induces the insulating behavior. It should apply to band, Mott [3], Anderson [9], quantum Hall [10], and possibly even to topological insulators. Therefore, it represents a promising approach to address the outstanding open problem of the fate of Anderson localization [11] in the presence of interactions [12–14].

So far, band and Mott insulators have been analyzed within the framework of the MTIS [3], both using lattice models in a tight-binding scheme, and also via *ab initio* electronic-structure simulations [9,15–18]. Instead, Anderson insulators have received little attention. In particular, it is not known, even for the noninteracting case, whether the many-body localization tensor may be used to locate the critical point of the (Anderson) transition which separates the conducting and the insulating phases in disordered systems.

The first purpose of the paper is to investigate this issue in the noninteracting case. With this aim, we study the Anderson transition in noninteracting one-dimensional lattice models close to half-filling. Since disorder correlations play a fundamental role in low-dimensional systems (for instance, they determine the presence or absence of transition points and mobility edges [19–21]), we consider various models of disorder and study the many-body localization tensor, and its reliability, in qualitatively different scenarios. First, like Ref. [9], we consider one-dimensional lattices with uncorrelated disorder, where the single-electron orbitals are expected to be exponentially localized at any nonzero disorder strength [11]. Then, we focus on the more intriguing and instructive case of deterministic disorder due to an external periodic potential whose period is incommensurate with the lattice. All single-particle orbitals of this Hamiltonian (named Aubry-André model) become localized, but only beyond a finite disorder strength [22]. Next, we consider a generalized Aubry-André model including next-nearest-neighbor hopping, where a mobility edge separating extended and localized single-particle orbitals was predicted [23]. Further, the case of nondeterministic disorder with tunable spatial correlations is addressed. In particular, we consider a one-dimensional lattice with a self-affine disordered potential, where both localized and extended single-particle orbitals were suggested to be present [24].

The second purpose of this paper is to investigate the effect of interactions on the Anderson transition. In particular, we consider spin-$\frac{1}{2}$ fermions in the Aubry-André model with onsite repulsive interactions. This model describes the experimental setup recently implemented with ultracold atomic gases in bichromatic optical lattices by the group of Bloch [25]. We employ the Hartree approximation with temperature-annealed

 ©2015 American Physical Society

self-consistent iterations to determine the phase boundary separating the metallic and the insulating ground states in the regime of weak interactions.

The paper is organized as follows: In Sec. II, we introduce the formalism of the MTIS, provide the definition of the many-body localization tensor, and describe our numerical procedure to compute it. The analysis of the one-dimensional Anderson model is reported in Sec. III. The Aubry-André model is analyzed in Sec. IV and the generalized Aubry-André model in Sec. V. The one-dimensional Anderson model with long-range correlated disorder is studied in Sec. VI. In Sec. VII, we address interaction effects in the Aubry-André model. In Sec. VIII, we draw the conclusions, focusing on the utility of the many-body localization tensor to identify conductor-insulator transitions in disordered systems with and without interactions.

II. LOCALIZATION TENSOR

In tune with Kohn's viewpoint on the origin of the insulating behavior, the authors of Ref. [3] provided a quantitative definition of the many-body localization tensor $\lambda_{\alpha\beta}$ (the indices α and β indicate spatial directions) rooted in the modern theory of polarization. This quantity measures the degree of localization of the particles in the many-body ground state and permits to discriminate metallic and insulating phases. In metals $\lambda_{\alpha\beta}$ is expected to be divergent in the thermodynamic limit, whereas it is finite in insulators; thus, it defines a many-body localization criterion for the ground state, referred to as Kohn's localization [9]. The formula for $\lambda_{\alpha\beta}$ was originally obtained from the estimator of the polarization [3], and can also be derived using a general geometric quantum theory [26]. The cases of periodic and open boundary conditions need to be treated separately because the position operator is ill defined in the former case [27].

In the case of periodic boundary conditions, the localization tensor is obtained through the auxiliary quantity $z_N^{(\alpha)}$, which for a system of N particles is defined as [3,26]

$$z_N^{(\alpha)} = \langle\Psi|e^{i\frac{2\pi}{L}\hat{\mathbf{R}}_\alpha}|\Psi\rangle, \tag{1}$$

where $|\Psi\rangle$ is the many-body ground state, $\hat{\mathbf{R}}_\alpha$ is the α component of the many-body position operator $\hat{\mathbf{R}} = \sum_{i=1}^{N}\hat{r}_i$, where $\hat{r}_i$ is the position operator for particle i, with the index $i = 1,\ldots,N$; L is the linear system size. We consider ground states of spin-$\frac{1}{2}$ fermions, with $N/2$ up and $N/2$ down spins. For noninteracting particles (or mean-field schemes such as restricted Hartree-Fock [28]), $z_N^{(\alpha)}$ may be further simplified, giving [26,28] $z_N^{(\alpha)} = \det^2[S_{jj'}^{(\alpha)}]$, where the matrix $[S_{jj'}^{(\alpha)}]$ (with the indices $j,j' = 1,2,\ldots N/2$) is the overlap matrix whose elements are given by

$$S_{jj'}^{(\alpha)} = \int d\mathbf{r}\,\phi_j^*(\mathbf{r})e^{i\frac{2\pi}{L}r_\alpha}\phi_{j'}(\mathbf{r}), \tag{2}$$

where $\phi_j(\mathbf{r})$ are the single-particle eigenstate spatial wave functions ordered for increasing energies, and $\mathbf{r}$ is the spatial coordinate. Using this auxiliary quantity, the localization tensor is now defined as [3,28]

$$\lambda_{\alpha\beta}^2 = -\frac{L^2}{4\pi^2 N}\ln\frac{|z_N^{(\alpha)}||z_N^{(\beta)}|}{|z_N^{(\alpha\beta)}|}, \tag{3}$$

where $z_N^{(\alpha\beta)}$ is defined as in Eq. (1) with R_α replaced by $R_\alpha - R_\beta$. In one-dimensional systems $N = L$ for half-filling, and the only component of the localization tensor is the one corresponding to $\alpha = \beta = x$, which is given by $\lambda_{xx}^2 = -L\ln|z_N|/2\pi^2$.

In the case of open boundaries, the position operator is well defined [27] and the localization tensor may be evaluated according to the formula [3,26]

$$\lambda_{\alpha\beta}^2 = (\langle\Psi|\hat{\mathbf{R}}_\alpha\hat{\mathbf{R}}_\beta|\Psi\rangle - \langle\Psi|\hat{\mathbf{R}}_\alpha|\Psi\rangle\langle\Psi|\hat{\mathbf{R}}_\beta|\Psi\rangle)/N. \tag{4}$$

For a system of independent electrons with $N/2$ spin-up and $N/2$ spin-down particles, this may be further simplified to give the squared localization length as [26]

$$\lambda_{\alpha\beta}^2 = \frac{1}{N}\int d\mathbf{r}\,d\mathbf{r}'(\mathbf{r}-\mathbf{r}')_\alpha(\mathbf{r}-\mathbf{r}')_\beta|P(\mathbf{r},\mathbf{r}')|^2, \tag{5}$$

where $\rho(\mathbf{r},\mathbf{r}') = 2P(\mathbf{r},\mathbf{r}')$ is the one-particle density matrix for a Slater determinant, which is given by [26]

$$\rho(\mathbf{r},\mathbf{r}') = 2\sum_{j=1}^{N/2}\phi_j(\mathbf{r})\phi_j^*(\mathbf{r}'). \tag{6}$$

We stress that the length scale λ_{xx} is a many-body localization length. In particular, it is not simply related to the spatial extent of the single-particle eigenstates. For example, in the case of noninteracting band insulators, λ_{xx} is related to the spread of the maximally localized Wannier functions [4], rather than to the Bloch wave functions. Notice that the latter (which are the single-particle eigenstates) are always extended. There is no simple analogy with the Wannier functions for the case of disordered systems.

Further insight into the nature of λ_{xx}^2 can be obtained via substitution of Eq. (6) into Eq. (5). In the one-dimensional case, one obtains the expression [16]

$$\lambda_{xx}^2 = \frac{2}{N}\sum_{i=1}^{N/2}[\langle\phi_i|\hat{x}^2|\phi_i\rangle - \langle\phi_i|\hat{x}|\phi_i\rangle^2] - \frac{2}{N}\sum_{i\neq j}|\langle\phi_i|\hat{x}|\phi_j\rangle|^2, \tag{7}$$

where $\hat{x}$ is the single-particle position operator. The first sum in this equation is proportional to the second moment of the single-particle orbitals. The second sum in Eq. (7) (which in the literature has been referred to as the covariance term [16]) originates from the antisymmetry of the many-particle wave function, and would be absent in a single-particle analysis. It reflects the correlations between different orbitals. These two sums are of the same order of magnitude, as confirmed by inspection of numerical results. In particular, in the localized phase they both contribute to the value of λ_{xx}^2, clearly indicating that this length scale reflects the properties of the many-particle wave function, even in noninteracting systems.

In generic insulators, including those with correlations, λ_{xx}^2 is related to measurable quantities such as the mean-square fluctuations of the polarization and the inverse of the optical

gap via a conductivity sum rule [4]. Furthermore, it is related to the spread of the generalized many-body Wannier functions, as defined in Ref. [4], which are localized in disconnected regions of the high-dimensional configuration space, establishing a direct connection with Kohn's theory of the insulating state.

The formulation to compute the localization length proposed in Refs. [3,26], and briefly summarized in this section, provides a computational procedure to verify Kohn's contention that the many-body ground state contains sufficient information to ascertain whether the system is an insulator or a conductor, without recourse to the analysis of low-lying excitations. In this paper, we provide evidence for a variety of disordered one-dimensional systems that this is indeed the case. The saturation of λ_{xx}^2 in the thermodynamic limit is taken to signal Kohn's localization [3,9], whereas its divergence indicates a conductor.

In our computations, we consider both periodic and open boundary conditions and employ, respectively, Eqs. (3) and (5) to compute the localization length. The single-particle spatial wave functions $\phi_j(\mathbf{r})$, needed to form the many-particle ground state, are determined from full diagonalization of the Hamiltonian matrix for a single spinless fermion using the Armadillo library [29].

III. 1D ANDERSON MODEL

We consider disordered tight-binding models of noninteracting spin-$\frac{1}{2}$ fermions defined by the Hamiltonian

$$H = t \sum_{r,\sigma} (b_{r,\sigma}^\dagger b_{r+1,\sigma} + \text{H.c}) + W \sum_{r,\sigma} \epsilon_r n_{r,\sigma}, \qquad (8)$$

where $r = 1, \ldots, L$ is the discrete index which labels the lattice sites, L is the linear system size, $b_{r,\sigma}$ ($b_{r,\sigma}^\dagger$) is the fermionic annihilation (creation) operator for a spin $\sigma = \uparrow, \downarrow$ particle at site r, and $n_{r,\sigma} = b_{r,\sigma}^\dagger b_{r,\sigma}$ is the corresponding particle number operator. Here and in the rest of the paper, the lattice spacing is used as the unit of length, and the (even) total number of fermions N is fixed. The hopping amplitudes to the nearest neighbors are set by t, ϵ_r is the (random) value of the energy at lattice site r, while the parameter W sets the strength of the disorder.

In this section we address, from a many-particle perspective, the Anderson model of localization where the onsite energies $\{\epsilon_r\}$ are sampled from a uniform probability distribution in the interval $[-1,+1]$.

For noninteracting many-particle systems in the ground state, the wave function is the Slater determinant formed with the lowest-energy occupied single-particle spin orbitals. The number of fermions per spin component determines the Fermi energy. In this paper, we consider the many-particle ground state of N spin-$\frac{1}{2}$ fermions, with $N/2$ spin-up and $N/2$ spin-down particles.

We recall that in one-dimensional (1D) systems with uncorrelated disorder, all single-particle orbitals are localized, meaning that they are characterized by an exponentially decaying envelope, for any nonzero disorder strength W. This follows from the one-parameter scaling theory [30], and was also shown more rigorously in Refs. [31,32]. According to Anderson's criterion of localization [11], which is based on the localized shape of the single-particle orbitals at the Fermi energy, the system should be an insulator at any filling.

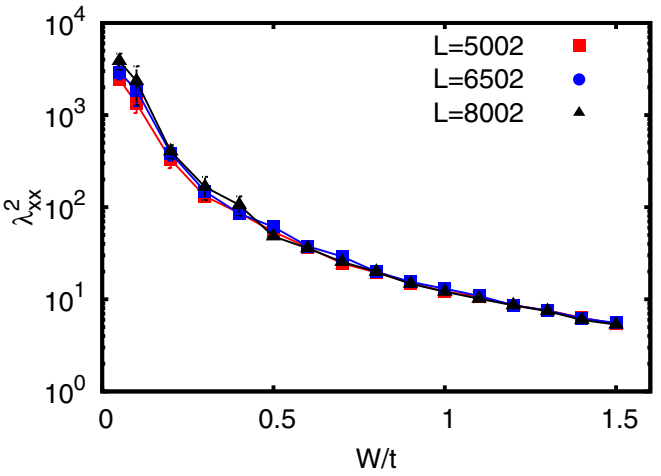

FIG. 1. (Color online) Half-filled 1D Anderson model with periodic boundary conditions: squared localization length λ_{xx}^2 (log-scale) as a function of the disorder strength W/t. Data for different systems sizes L are shown, and their mutual agreement indicates Kohn's localization at all disorder strengths. The lines are guides to the eye. Here and in all figures, the unit of length is the lattice spacing.

In Fig. 1, we show the results for the squared localization tensor λ_{xx}^2 as a function of the disorder strength W/t. The data corresponding to three large (even) lattice sizes with periodic boundary conditions are shown. The lattices are half-filled, and ensemble averaging of the results is performed considering 5–10 realizations of the disorder pattern. The localization length λ_{xx} varies by a few orders of magnitude as we tune the disorder strength. However, it is always finite and system-size independent, in the whole range of disorder strengths we explore, which extends down to the extremely weak disorder $W/t = 0.05$. These findings constitute a clear signature of Kohn's localization. Also, the variation of λ_{xx}^2 with the disorder strength exhibits no sharp features (as opposed to the results of the next sections). We verified that the data obtained using open boundary conditions (not shown) agree with those obtained using periodic boundary conditions.

Therefore, we conclude that the formalism of the MTIS predicts the many-particle ground state of the 1D Anderson model to be an insulator, in agreement with the theory of Anderson localization and the one-parameter scaling theory [30]. However, in this latter formalism, the insulating character is attributed to the localized shape of the single-particle orbitals in the vicinity of the Fermi energy, while the MTIS deals with the many-body ground-state wave function.

IV. AUBRY-ANDRÉ MODEL

In this section, we consider the one-dimensional Aubry-André model [22]. This is described by the Hamiltonian defined in Eq. (8), but with the onsite energies given by the incommensurate potential $\epsilon_r = \cos(2\pi r g + \theta)$, where $g = (\sqrt{5}+1)/2$ is the golden ratio, and θ is an (almost) arbitrary phase. This is an archetypal model to study Anderson transitions in lower dimensions; it has been experimentally

realized with ultracold atomic gases trapped in bichromatic optical lattices [33], and also in quasiperiodic photonic lattices [34].

The sinusoidal potential does not display periodicity on a finite lattice, and so the Aubry-André model is, in this sense, disordered. However, this disorder is deterministic, and so is not truly random. In the presence of such "deterministic disorder," as opposed to true disorder, the one-parameter scaling theory of Ref. [30] does not apply. In fact, it is known that this model hosts a transition from a diffusive phase at weak disorder to a localized phase at strong disorder. In the former phase, all single-particle eigenstates are extended over the whole system (possibly with the exception of a zero-measure set of nonexponentially localized states) [22]. In the latter phase, they are all localized if g is a Diophantine number (which is the case considered here) and for almost every value of θ [35]. We chose $\theta = 0$. The transition occurs at the critical disorder strength $W_c/t = 2$.

In simulations with periodic boundary conditions, we need to consider system sizes given by Fibonacci numbers, so that the potential fits the periodicity of the lattice. The results for the squared localization length λ^2_{xx} of half-filled lattices are displayed in Fig. 2 (top panel), both for periodic and open boundary conditions. A sharp variation of λ^2_{xx} occurs in the close vicinity of $W/t = 2$. For $W/t > 2$, the localization length is finite and does not depend on the system size. This is a signature of Kohn's localization. Instead, for $W/t < 2$, a very rapid increase of λ^2_{xx} with the system size is observed, possibly indicating a metallic phase. In order to confirm this supposition, we perform a detailed analysis of the finite-size scaling of λ^2_{xx}. Various data sets obtained in the regime $W < 2$ are shown in Fig. 2 (bottom panel). A best-fits analysis indicates that these data are accurately described by the (empirical) power-law fitting functions: $\lambda^{-2}_{xx} = cL^{-\gamma}$, where c and γ are the fitting parameters. The exponents obtained from the fitting procedure are $\gamma = 1.135(2), 1.151(2), 1.14(1)$ (for $W/t = 0.2, 0.5, 1$), and $\gamma = 1.008(5)$ ($W/t = 1$) for periodic and open boundary conditions, respectively. This fitting function predicts a divergence of the many-body localization length in the thermodynamic limit, providing a clear indication of metallic behavior. The divergence occurs both for periodic and open boundary conditions, but it is more rapid in the former case.

It is worth noticing that in the insulating phase the values of λ^2_{xx} obtained using periodic and open boundary conditions are indistinguishable within our numerical accuracy. This independence from the type of boundary conditions is indeed expected for insulators since in these systems the localization lengths (and the polarization) are bulk properties, as opposed to metals where they depend on the size of the system.

The analysis of the Aubry-André model in the framework of the MTIS provides a clear signature of the metal-insulator transition at $W/t = 2$, in agreement with the Anderson criterion of localization, which also predicts a phase transition at the same disorder strength since the single-particle orbitals change from extended to localized [22]. We point out that we also performed a similar analysis of the Aubry-André model at different lattice fillings in the regime $0.1 < N/(2L) < 0.9$, without observing measurable shifts of the critical point. This is also expected following Anderson's criterion of localization since the single-particle spectrum of this model does not host mobility edges [22].

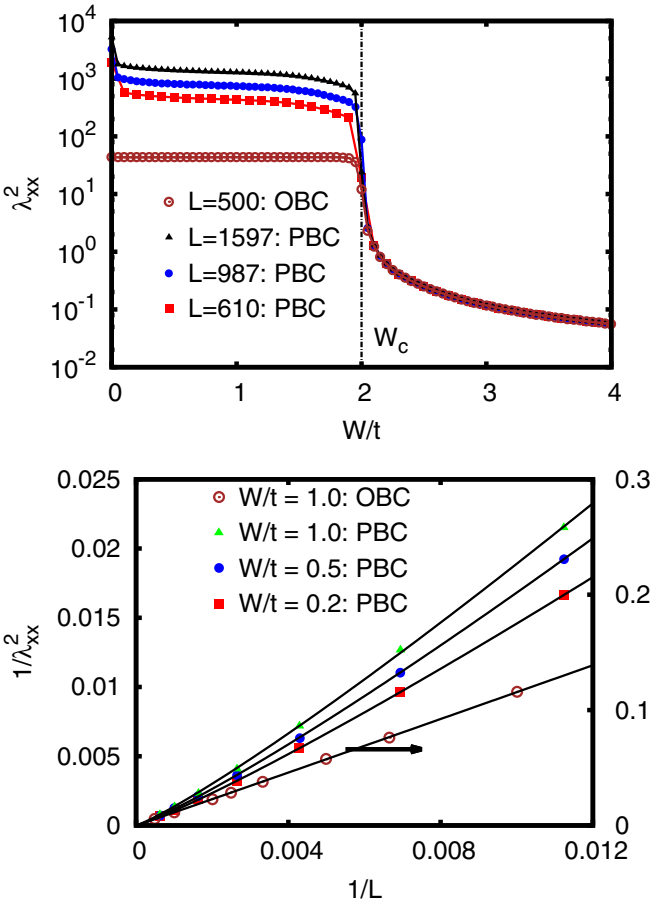

FIG. 2. (Color online) Half-filled 1D Aubry-André model. Top panel: squared localization length λ^2_{xx} (log-scale) as a function of the quasidisorder strength W/t for periodic (PBC) and open (OBC) boundary conditions, and for different Fibonacci lengths L of the chain; the vertical line indicates the critical disorder strength $W_c/t = 2$, separating extended from localized states. Bottom panel: scaling of λ^{-2}_{xx} with the inverse system size $1/L$ in the conducting phase $W_c/t < 2$. The continuous curves represent the power-law fits $\lambda^{-2}_{xx} = cL^{-\gamma}$ (c and γ are fitting parameters). λ^{-2}_{xx} diverges with the exponent $\gamma \approx 1.14$ for PBC (left axis) and with $\gamma = 1.008(5)$ for OBC (right axis).

V. GENERALIZED AUBRY-ANDRÉ MODEL

Hopping processes beyond nearest-neighbor sites can dramatically alter the localization properties, even causing the occurrence of single-particle mobility edges when none existed in the absence of such effects [23]. In this section, we consider the generalized Aubry-André model, including next-nearest-neighbor hopping. With this modification, one obtains the Hamiltonian $H' = H + t_2 \sum_{r,\sigma} (b^\dagger_{r,\sigma} b_{r+2,\sigma} + \text{H.c})$, where H is defined in Eq. (8), t_2 is the energy associated to hopping to next-nearest neighbors, and the onsite energies $\epsilon_{\mathbf{r}}$ are defined by the same incommensurate sinusoidal potential of the native Aubry-André model considered in the previous section.

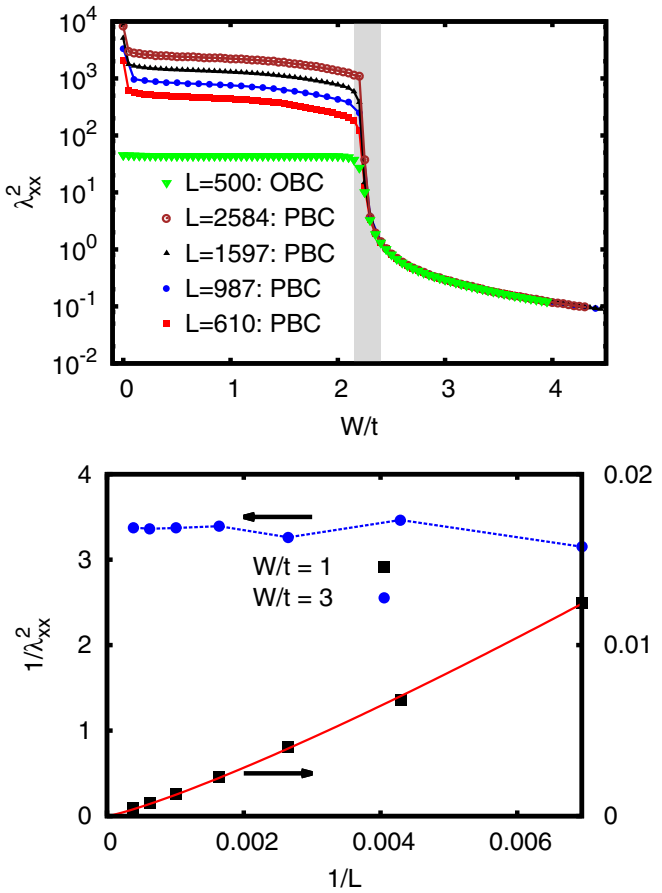

FIG. 3. (Color online) Generalized 1D Aubry-André model with next-nearest hopping $t_2/t = 0.5$, at half-filling. Top panel: squared localization length λ_{xx}^2 (log-scale) as a function of the quasidisorder strength W/t. Data for periodic (PBC) and open boundary conditions (OBC) are shown for different chain lengths L. The gray vertical stripe indicates the approximate location of the critical point between the metallic and the insulating phases. Bottom panel: scaling of inverse squared localization length $1/\lambda_{xx}^2$ with the inverse system size $1/L$ at quasidisorder strength in the metallic phase $W/t = 1$ and in the insulating phase $W/t = 3$ (blue dashed lines are a guide to eye). The continuous red curve represents the power-law fitting function $\lambda_{xx}^{-2} = cL^{-\gamma}$, with the best-fit parameter $\gamma = 1.19(2)$.

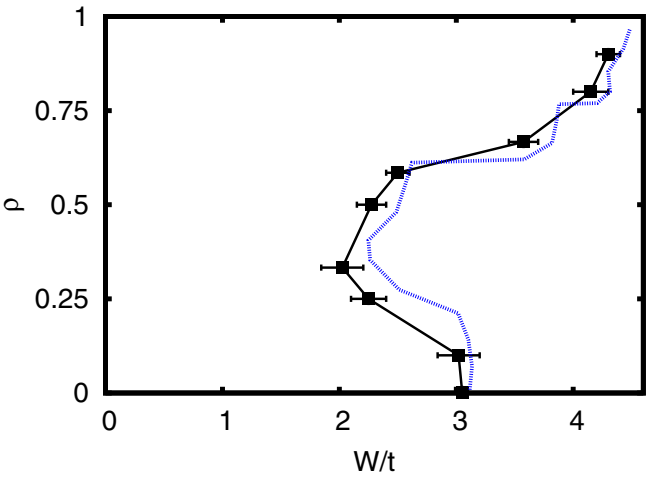

FIG. 4. (Color online) Zero-temperature phase diagram of the generalized Aubry-André model with $t_2/t = 0.5$, as a function of filling $\rho = N/(2L)$ and quasidisorder strength W/t. The black points indicate the phase boundary separating the metallic phase (left) from the insulating phase (right) obtained within the MTIS. Our results may be compared with the critical point extracted from the inverse participation data of Ref. [23] (blue dashed curve).

This generalized Aubry-André model was studied in Ref. [23]. The analysis of the single-particle spectrum based on calculations of the inverse participation ratio (which measures the spatial extent of the single-particle orbitals) presented evidence of the presence of mobility edges in a certain regime of disorder strength W. The location of the mobility edges was found to vary with W. As in previous sections, here we analyze the many-particle ground state of the generalized Aubry-André Hamiltonian in the framework of the MTIS. We consider various lattice fillings, varying from vanishing density to full filling. We fix the next-nearest-neighbor hopping at $t_2/t = 0.5$, a value which was also considered in Ref. [23]. An illustrative example of the dependence of the squared localization length λ_{xx}^2 as a function of W is shown in Fig. 3 (top panel), where the data sets correspond to half-filled lattices of different sizes L. Here too, as in the case of the native Aubry-André model, a sharp variation of λ_{xx} occurs at a finite disorder strength W_c. For $W > W_c$, λ_{xx}^2 is finite and system-size independent, indicating Kohn's localization. Instead, for $W < W_c$, λ_{xx}^2 rapidly increases as L increases. In order to assert whether in this regime the ground state is metallic, we analyze the finite-size scaling of λ_{xx}^2 [see Fig. 3 (bottom panel)]. The scaling of the squared localization length with the system size L turns out to be accurately described by the empirical fitting function $\lambda_{xx}^{-2} = cL^{-\gamma}$, where c and γ are fitting parameters. At $W/t = 1$, the best fit is obtained with $\gamma = 1.19(2)$. This scaling behavior clearly indicates a divergence of the localization length, which is a signature of metallic behavior.

In order to approximately pinpoint the phase boundary between the metal and the insulator, we determine the largest disorder strength where λ_{xx} clearly diverges in the thermodynamic limit, and the smallest value of W where it is system size independent, within numerical accuracy. This allows us to provide a (rather narrow) interval containing the critical disorder strength W_c. For the case of half-filling, we obtain $W_c/t = 2.275 \pm 0.125$. This is displayed in Fig. 3 (top panel) as a gray vertical stripe.

By performing a similar analysis for different fillings, we obtain the zero-temperature phase diagram as a function of disorder strength and filling factor $\rho = N/(2L)$ (see Fig. 4). The phase boundary separating the metallic and the insulating phases varies rapidly with the filling. Interestingly, these variations are nonmonotonic: starting from the zero-density limit, W_c first decreases as the filling increases, then it rapidly increases when the filling is $\rho \gtrsim 0.5$.

These findings obtained within the MTIS can be compared with the prediction based on the Anderson criterion of localization. We extract the location of the single-particle mobility edge from the contour plot data of the inverse participation ratio provided in Ref. [23]. This procedure is based on the digitalization of the color scale shown in Ref. [23], and so it

entails some approximations. Vanishing values of the inverse participation ratio indicate extended single-particle orbitals, while finite values indicate localized states. The critical filling factor is obtained when the Fermi energy reaches the mobility edge. Notice that in Ref. [23] only the single lattice size $L = 500$ was considered, without analyzing the finite-size scaling behavior. From the scattering of their data for $L = 500$, we estimate the indeterminacy on the extracted critical filling to be close to 10%. Therefore, performing a precise quantitative comparison between our data and those of Ref. [23] may not be completely justified. However, we see from Fig. 4 that the overall agreement is good. In particular, certain important features of the ground-state phase diagram are predicted by both theories. First, in the low-filling limit both theories predict the critical disorder to be $W_c/t \simeq 3$, significantly larger than in the native Aubry-André model (where $W_c/t = 2$). Second, the location of the phase boundary has large nonmonotonic variations as a function of the filling factor.

VI. 1D ANDERSON MODEL WITH CORRELATED DISORDER

The properties of the Anderson model defined in Sec. III are affected in a nontrivial manner by the presence of spatial correlations in the disorder pattern, in particular if the correlations have a long-range character [19,24,36,37].

The effect of long-range spatial correlations has been investigated in several studies, considering in particular disorder patterns characterized by a power-law spectral density $S(k) \propto k^{-\alpha}$, where $S(k)$ is the Fourier transform of the two-point correlation function $\langle \epsilon_r \epsilon_{r'} \rangle$, and the brackets $\langle \ldots \rangle$ indicate spatial averaging. The value of the exponent α determines the extent of the spatial correlations. The case $\alpha = 0$ corresponds to uncorrelated disorder. For $\alpha > 2$, one has energy sequences with persistent increments [24].

A disorder pattern with power-law spectral density can be constructed using the following equation [24]:

$$\epsilon_r = \sum_{k=1}^{L/2} (k^{-\alpha}[2\pi/L]^{1-\alpha})^{1/2} \cos(2\pi r k/L + \phi_k), \qquad (9)$$

where ϕ_k (with $k = 1, \ldots L/2$) are random phases sampled from a uniform distribution in the range $[0,2\pi]$. In our calculations, we shift the onsite energies in order to obtain a disorder pattern with zero mean [24]: $\epsilon_{\rm ave} = \sum_r \epsilon_r = 0$. Also, in order to curtail the growth of the disorder fluctuations as the system size increases, it is necessary to fix the magnitude of the variance of the onsite energies at $\sum_r (\epsilon_r - \epsilon_{\rm ave})^2 = 1$, by appropriately rescaling the onsite energy distribution [24]. Notice that, in the notation of Eq. (8), the disorder-strength parameter is fixed at $W/t = 1$. This value is not equal to the maximum amplitude of the onsite random potential. This model of correlated disorder is nondeterministic, and so it differs in nature from the deterministic disorder of the Aubry-André models described in Secs. IV and V. However, its properties are also qualitatively different compared to the uncorrelated Anderson model of Sec. III.

In fact, a renormalization group study [24] predicted that for large exponents $\alpha > \alpha_c = 2$ the single-particle orbitals become extended in a finite portion of the energy spectrum close to the band center. This is in sharp contrast with the case of uncorrelated disorder, where all single-particle orbitals are localized in one-dimensional systems [30–32]. It is worth emphasizing that the rescaling of the onsite energies was found to be crucial for the occurrence of the single-particle extended states [38–40].

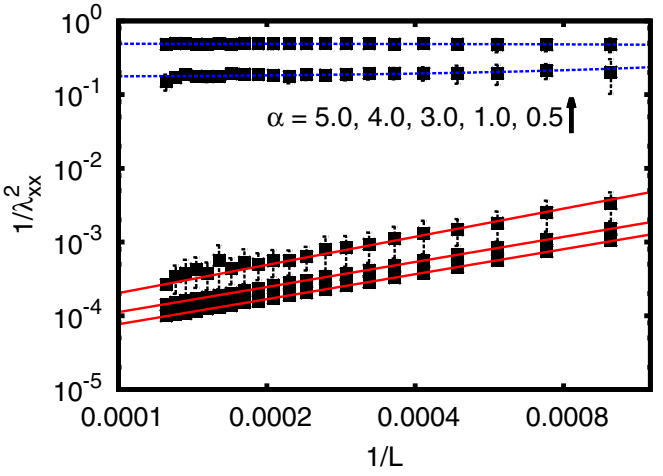

FIG. 5. (Color online) Half-filled 1D Anderson model with long-range correlated disorder and PBC: scaling of ensemble-averaged inverse squared localization length $1/\lambda^2_{xx}$ as a function of the inverse chain length $1/L$ (log-log scale), for various values of the exponent α characterizing the disorder spectral density. For $\alpha = 3.0,4.0,5.0$ our simulations indicate a divergence of λ^2_{xx} with system size, which is accurately described by the power-law fitting function $\lambda^{-2}_{xx} = cL^{-\gamma}$ (c and γ are fitting parameters), shown as red solid lines. For $\alpha = 0.5,1$ the results suggest a saturation of λ^2_{xx} in the thermodynamic limit; the blue dotted lines indicate linear fits.

Figure 5 reports the squared localization length λ^2_{xx} in half-filled chains for various values of the exponent α. The data points correspond to ensemble averages obtained using from 10 to 200 realizations of the disorder pattern. The error bars represent the standard deviation of the population (instead of the estimated standard deviation of the average) since, as pointed out in Ref. [41], in the presence of long-range correlations sample-to-sample fluctuations survive in the thermodynamic limit.

As seen from the log-log scale of Fig. 5, the data sets corresponding to large exponents $\alpha > \alpha_c$ display a clear power-law divergence of the localization length λ_{xx} with the system size, indicating metallic behavior in the many-particle system. Similarly to previous sections, we fit the disorder-averaged data for $\alpha > 2$ with the fitting function $\lambda^{-2}_{xx} = cL^{-\gamma}$. The best fits are obtained with the exponents $\gamma = 1.26(3),1.130(4),1.127(4)$, for $\alpha = 3.0,4.0,5.0$, respectively. Notice that the latter two data are close to the values found for the Aubry-André model in the metallic phase. In contrast, for lower values of $\alpha < 2$ λ saturates with the increase of system size. This is confirmed by performing linear fits which extrapolate to finite values in the thermodynamic limit. These findings are consistent with the single-particle analysis of Ref. [24]. Indeed, at half-filling the Fermi energy is close to the band center, where the extended single-particle orbitals have been predicted to occur. Notice that, according to

Ref. [41], ensemble averaging causes the transition between single-particle localized and delocalized states to morph into a crossover. However, our aim here is only to identify the two many-particle regimes with metallic and insulating phases, without focusing on the precise location of the transition point. In fact, we have checked that the two phases (with, respectively, diverging and saturating localization lengths) can be unambiguously identified also by analyzing the data corresponding to single realizations (not shown).

Our study, from the many-particle perspective of the MTIS, substantiates the claim made in Ref. [24] vis-à-vis the occurrence of metallic states in 1D.

VII. INTERACTING AUBRY-ANDRÉ MODEL

Understanding the intricate interplay between disorder and interactions in many-fermion systems is an outstanding open problem [42]. In particular, it is still unclear how an Anderson localized system is affected when electron-electron interactions are included [12,14]. The MTIS is clearly a promising approach to address this problem, given that it allows us to describe both noninteracting and interacting insulators within the same formalism.

Here, we investigate the effect of weak repulsive interactions in the Aubry-André model. The Hamiltonian we consider is defined as

$$H_{\rm int} = H + U \sum_r n_{r,\uparrow} n_{r,\downarrow}, \tag{10}$$

where H is the noninteracting Hamiltonian defined in Eq. (8), with the incommensurate disorder pattern ϵ_r employed in Sec. IV. The parameter $U \geq 0$ characterizes the interaction strength, while $n_{r,\uparrow}$ ($n_{r,\downarrow}$) is the spin-up (spin-down) density operator at site r. This Hamiltonian describes the experimental setup recently implemented by the group of Bloch [25]. The experimenters created quasi-one-dimensional tubes with two standing laser waves along the axial direction. One of the two lasers has a period which is incommensurate with the other. This creates the deterministic disorder pattern ϵ_r characterizing the Aubry-André model. The interaction strength U can be tuned employing a Feshbach resonance.

Our goal is to determine the zero-temperature phase diagram of the Hamiltonian (10) at half-filling $N = L$, in the regime of weak interactions. We restrict our analysis to paramagnetic phases (allowing charge-density waves), and we determine the phase boundary separating the metallic and the insulating ground states. In the regime of relatively strong disorder and weak interactions, the Hartree approximation is expected to provide reliable results [43,44]. Within this approximation, the Hamiltonian (10) is simplified using a mean-field decoupling of the interaction term, obtaining

$$\begin{aligned} H_{\rm int} &\approx H^{{\rm MF},\uparrow} + H^{{\rm MF},\downarrow} + I, \\ H^{{\rm MF},\uparrow} &= H^{\uparrow} + U \sum_i \langle n_{r,\downarrow}\rangle n_{r,\uparrow}, \\ H^{{\rm MF},\downarrow} &= H^{\downarrow} + U \sum_i \langle n_{r,\uparrow}\rangle n_{r,\downarrow}, \\ I &= -U \sum_r \langle n_{r,\uparrow}\rangle \langle n_{r,\downarrow}\rangle, \end{aligned} \tag{11}$$

where H^{σ} is that part of $H = H^{\uparrow} + H^{\downarrow}$ corresponding to spin $\sigma = \uparrow, \downarrow$. The densities are obtained via a self-consistent iterative procedure based on the equation $\langle n_{r,\sigma}\rangle = \sum_{\alpha=1}^{N/2} Q^{(\sigma)*}_{r,\alpha} Q^{(\sigma)}_{r,\alpha}$, where $Q^{(\sigma)}$ is the matrix of eigenvectors of the mean-field Hartree Hamiltonians $H^{{\rm MF},\sigma}$. Paramagnetism is enforced by setting $\langle n_{r,\uparrow}\rangle = \langle n_{r,\downarrow}\rangle$. Special care has to be taken in order to ensure that the iterative procedure converges to the true ground state; following Ref. [44], we implemented an annealing scheme where a fictitious temperature parameter is gradually reduced down to zero temperature. This temperature-annealing scheme is combined with the standard damping of the density profile provided by each iteration. The Hartree formalism is based on an ansatz that the ground state is a Slater determinant, which allows us to compute λ^2_{xx} as described in Sec. II [28].

Our main results are presented in Fig. 6. The left panel shows the squared localization length λ^2_{xx} as a function of disorder strength W for various interaction strengths; the sharp jump in λ^2_{xx} signals the conductor-insulator transition. In the conducting phase, the localization length is cut off by the system size and is independent of the interaction strength. The inset of the right panel of Fig. 6 shows the scaling of λ^{-2}_{xx} with inverse system size for $U/t = 0.3$, at two disorder strengths $W/t = 2.3, 2.7$; for the latter value we see that, in the thermodynamic limit, λ^2_{xx} saturates (signaling an insulator) whereas it diverges for the former (signaling a conductor).

An accurate estimate of the transition point is obtained by locating the maximum differential of a polynomial function which fits the data of λ^2_{xx} as a function of W. With this procedure, we determine the zero-temperature paramagnetic phase diagram of the weakly interacting Aubry-André model, shown in the right panel of Fig. 6. There is a linear increase of the critical disorder separating the metallic and the insulating (paramagnetic) phases. This indicates that repulsive interactions induce delocalization. It is worth mentioning that a positive drift of the critical disorder strength has been obtained also in earlier theoretical studies of the Mott-Anderson transition in higher dimensions based on dynamical mean-field theory [45]. An interaction-induced increase of the localization length was also previously seen in a one-dimensional Anderson-Hubbard model within a simple mean-field treatment valid in the atomic limit [46]; however, no metallic transition was observed in that study. In recent experiments, a small linear increase of the critical disorder strength was observed in a three-dimensional disordered optical lattice [47]. Moreover, the bosonic interacting Aubry-André model was implemented in Ref. [48], where interaction-induced delocalization was again observed. Bloch's group implemented the fermionic interacting Aubry-André model [25], and determined the critical disorder strength where many-body localization, which is a dynamical phase transition taking place at finite-energy density, occurs. The critical disorder strength was found to increase as a function of the interaction strength for weak interactions, echoing our findings for the ground state. We propose that the ground-state metal-insulator transition could be observed in their setup by employing the technique used in Refs. [47,49], where an effective force is imposed on the atoms either by shifting the harmonic confinement or by applying

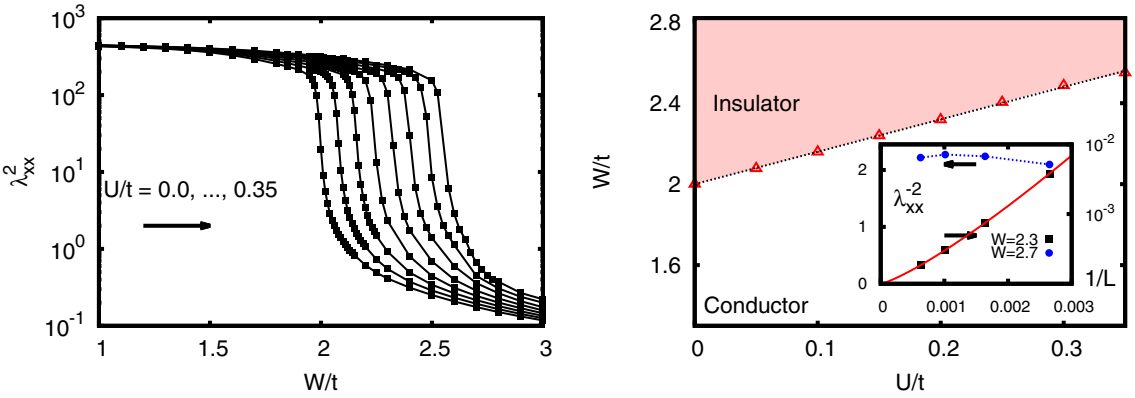

FIG. 6. (Color online) Interacting Aubry-André model at half-filling. Left panel: squared localization length λ^2_{xx} for a periodic chain of length $L = 610$ for various interaction strengths U; the jump in λ^2_{xx} signals the conductor-insulator transition. Right panel: paramagnetic ground-state phase diagram showing the dependence of critical disorder W_c separating insulating and conducting phases as a function of weak interactions U. Inset shows scaling of λ^{-2}_{xx} with inverse system length L for $U/t = 0.3$ at two fixed disorder strengths $W/t = 2.3,2.7$; the scaling behavior clearly signals an insulator for the latter and a conductor for the former.

a magnetic field gradient; such experimental results could directly be compared with our phase diagram.

VIII. CONCLUSIONS

Developing approaches to locate insulating transitions in disordered systems, for noninteracting or interacting systems, at zero or finite temperatures, is a central problem in condensed matter physics and a subject of intense research [12–14,50–52]. In this paper, we addressed the zero-temperature aspects of this problem from the perspective of the MTIS. Our findings provide evidence that the many-body localization tensor, a bulk quantity measuring Kohn's localization, provides a clear signature of the insulating transition induced by disorder at zero temperature. This was first verified in noninteracting one-dimensional models with uncorrelated disorder, deterministic disorder due to incommensurate potentials, and disorder with long-range correlations described by a power-law spectral function.

In particular, it was verified that the ground state of the one-dimensional Anderson model is insulating at any disorder strength, in agreement with the one-parameter scaling theory [30] of Anderson localization. In the cases of deterministic and correlated disorder, we found evidence of metal-insulator transitions, in agreement with previous studies on the critical disorder strength and on the position of the mobility edge based on single-particle theories.

Finally, we investigated the conductor-insulator transition in a disordered interacting system: Using the Hartree mean-field analysis within the MTIS, we found that weak repulsive interactions induce delocalization in the paramagnetic ground state of the Aubry-André model at half-filling, leading to an increase of the critical disorder strength required for the onset of insulating behavior. These findings could be observed in cold atoms using available experimental techniques [25,47,49].

One very appealing feature of the present approach is that it permits to identify the insulating phase using only ground-state properties. On the other hand, alternative approaches to identifying the insulating state, such as the Kubo formula for dc conductivity, require the knowledge of, at the very least, low-lying excited states. Within the MTIS, the knowledge of the ground-state many-particle wave function alone suffices, a feature which makes it suitable for large-scale computational approaches such as, say, quantum Monte Carlo simulations [17,18].

ACKNOWLEDGMENTS

We acknowledge insightful comments from R. Resta on the manuscript, help from M. Atambo with computing facilities, related collaboration with G. Gebreyesus, and interesting discussions with T. Nguyen and J. Goold.

[1] W. Kohn, Phys. Rev. **133**, A171 (1963).
[2] W. Kohn, in *Many-Body Physics*, edited by C. DeWitt and R. Balian (Gordon and Breach, New York, 1968).
[3] R. Resta and S. Sorella, Phys. Rev. Lett. **82**, 370 (1999).
[4] I. Souza, T. Wilkens, and R. M. Martin, Phys. Rev. B **62**, 1666 (2000).
[5] N. Marzari and D. Vanderbilt, Phys. Rev. B **56**, 12847 (1997).
[6] R. D. King-Smith and D. Vanderbilt, Phys. Rev. B **47**, 1651 (1993).
[7] R. Resta and D. Vanderbilt, *Physics of Ferroelectrics*, Vol. 105 of Topics in Applied Physics (Springer, Berlin, 2007), pp. 31–68.
[8] N. A. Spaldin, J. Solid State Chem. **195**, 2 (2012).
[9] G. L. Bendazzoli, S. Evangelisti, A. Monari, and R. Resta, J. Chem. Phys. **133**, 064703 (2010).
[10] R. Resta, Phys. Rev. Lett. **95**, 196805 (2005).
[11] P. W. Anderson, Phys. Rev. **109**, 1492 (1958).
[12] I. V. Gornyi, A. D. Mirlin, and D. G. Polyakov, Phys. Rev. Lett. **95**, 206603 (2005).

[13] L. Fleishman and P. W. Anderson, Phys. Rev. B **21**, 2366 (1980).
[14] D. M. Basko, I. L. Aleiner, and B. L. Altshuler, Ann. Phys. (NY) **321**, 1126 (2006).
[15] V. Vetere, A. Monari, G. L. Bendazzoli, S. Evangelisti, and B. Paulus, J. Chem. Phys. **128**, 024701 (2008).
[16] M. Veithen, X. Gonze, and P. Ghosez, Phys. Rev. B **66**, 235113 (2002).
[17] N. D. M. Hine and W. M. C. Foulkes, J. Phys.: Condens. Matter **19**, 506212 (2007).
[18] L. Stella, C. Attaccalite, S. Sorella, and A. Rubio, Phys. Rev. B **84**, 245117 (2011).
[19] F. M. Izrailev and A. A. Krokhin, Phys. Rev. Lett. **82**, 4062 (1999).
[20] D. H. Dunlap, K. Kundu, and P. Phillips, Phys. Rev. B **40**, 10999 (1989).
[21] B. Pal, S. K. Maiti, and A. Chakrabarti, Europhys. Lett. **102**, 17004 (2013).
[22] S. Aubry and G. André, Ann. Isr. Phys. Soc. **3**, 133 (1980).
[23] J. Biddle, D. J. Priour, B. Wang, and S. Das Sarma, Phys. Rev. B **83**, 075105 (2011).
[24] F. A. B. F. de Moura and M. L. Lyra, Phys. Rev. Lett. **81**, 3735 (1998).
[25] M. Schreiber, S. S. Hodgman, P. Bordia, H. P. Lüschen, M. H. Fischer, R. Vosk, E. Altman, U. Schneider, and I. Bloch, Science **349**, 842 (2015).
[26] R. Resta, Eur. Phys. J. B **79**, 121 (2011).
[27] R. Resta, Phys. Rev. Lett. **80**, 1800 (1998).
[28] R. Resta, J. Phys.: Condens. Matter **14**, R625 (2002).
[29] C. Sanderson, Technical Report NICTA, 2010 (unpublished).
[30] E. Abrahams, P. W. Anderson, D. C. Licciardello, and T. V. Ramakrishnan, Phys. Rev. Lett. **42**, 673 (1979).
[31] I. Y. Gol'dsheĭdt, S. A. Molchanov, and L. A. Pastur, Funktsional. Anal. Prilozh. **11**, 1 (1977).
[32] I. M. Lifshits, S. A. Gredeskul, and L. A. Pastur, *Introduction to the Theory of Disordered Systems* (Wiley, New York, 1982).
[33] G. Roati, C. D'Errico, L. Fallani, M. Fattori, C. Fort, M. Zaccanti, G. Modugno, M. Modugno, and M. Inguscio, Nature (London) **453**, 895 (2008).
[34] Y. Lahini, R. Pugatch, F. Pozzi, M. Sorel, R. Morandotti, N. Davidson, and Y. Silberberg, Phys. Rev. Lett. **103**, 013901 (2009).
[35] S. Y. Jitomirskaya, Ann. Math. **150**, 1159 (1999).
[36] C. M. Soukoulis, M. J. Velgakis, and E. N. Economou, Phys. Rev. B **50**, 5110 (1994).
[37] A. Croy, P. Cain, and M. Schreiber, Eur. Phys. J. B **82**, 107 (2011).
[38] J. W. Kantelhardt, S. Russ, A. Bunde, S. Havlin, and I. Webman, Phys. Rev. Lett. **84**, 198 (2000).
[39] F. A. B. F. de Moura and M. L. Lyra, Phys. Rev. Lett. **84**, 199 (2000).
[40] S. Russ, J. W. Kantelhardt, A. Bunde, and S. Havlin, Phys. Rev. B **64**, 134209 (2001).
[41] S. Nishino, K. Yakubo, and H. Shima, Phys. Rev. B **79**, 033105 (2009).
[42] B. L. Altshuler and A. G. Aronov, in *Electron-Electron Interactions in Disordered Systems*, edited by A. L. Efros and M. Pollak (North-Holland, Amsterdam, 1985).
[43] P. Fazekas, *Lecture Notes on Electron Correlation and Magnetism* (World Scientific, Singapore, 1999).
[44] D. C. Cabra and G. L. Rossini, Phys. Rev. B **69**, 184425 (2004).
[45] K. Byczuk, W. Hofstetter, and D. Vollhardt, Phys. Rev. Lett. **94**, 056404 (2005).
[46] P. Henseler, J. Kroha, and B. Shapiro, Phys. Rev. B **77**, 075101 (2008).
[47] S. S. Kondov, W. R. McGehee, W. Xu, and B. DeMarco, Phys. Rev. Lett. **114**, 083002 (2015).
[48] B. Deissler, M. Zaccanti, G. Roati, C. D'Errico, M. Fattori, M. Modugno, G. Modugno, and M. Inguscio, Nat. Phys. **6**, 354 (2010).
[49] L. Tanzi, E. Lucioni, S. Chaudhuri, L. Gori, A. Kumar, C. D'Errico, M. Inguscio, and G. Modugno, Phys. Rev. Lett. **111**, 115301 (2013).
[50] G. Schubert, J. Schleede, K. Byczuk, H. Fehske, and D. Vollhardt, Phys. Rev. B **81**, 155106 (2010).
[51] C. E. Ekuma, H. Terletska, K.-M. Tam, Z.-Y. Meng, J. Moreno, and M. Jarrell, Phys. Rev. B **89**, 081107 (2014).
[52] V. Oganesyan and D. A. Huse, Phys. Rev. B **75**, 155111 (2007).